AIP | The Journal of Chemical Physics

Molecular dynamics simulation of the polymer electrolyte poly(ethylene oxide)/ Li Cl O 4 . II. Dynamical properties

Leonardo J. A. Siqueira and Mauro C. C. Ribeiro

Citation: The Journal of Chemical Physics **125**, 214903 (2006); doi: 10.1063/1.2400221
View online: http://dx.doi.org/10.1063/1.2400221
View Table of Contents: http://scitation.aip.org/content/aip/journal/jcp/125/21?ver=pdfcov
Published by the AIP Publishing

THE JOURNAL OF CHEMICAL PHYSICS **125**, 214903 (2006)

Molecular dynamics simulation of the polymer electrolyte poly(ethylene oxide)/$LiClO_4$. II. Dynamical properties

Leonardo J. A. Siqueira and Mauro C. C. Ribeiro[a]
Laboratório de Espectroscopia Molecular, Instituto de Química, Universidade de São Paulo, C.P. 26077, CEP 05513-970 São Paulo, SP, Brazil

(Received 6 July 2006; accepted 27 October 2006; published online 5 December 2006)

The dynamical properties of the polymer electrolyte poly(ethylene oxide) (PEO)/$LiClO_4$ have been investigated by molecular dynamics simulations. The effect of changing salt concentration and temperature was evaluated on several time correlation functions. Ionic displacements projected on different directions reveal anisotropy in short-time (rattling) and long-time (diffusive) dynamics of Li^+ cations. It is shown that ionic mobility is coupled to the segmental motion of the polymeric chain. Structural relaxation is probed by the intermediate scattering function $F(\mathbf{k},t)$ at several wave vectors. Good agreement was found between calculated and experimental $F(\mathbf{k},t)$ for pure PEO. A remarkable slowing down of polymer relaxation is observed upon addition of the salt. The ionic conductivity estimated by the Nernst-Einstein equation is approximately ten times higher than the actual conductivity calculated by the time correlation function of charge current. © *2006 American Institute of Physics*. [DOI: 10.1063/1.2400221]

I. INTRODUCTION

Polymer electrolytes are used in the technology of lithium ion battery as solid-state electrolytes.[1–5] Usually, they are synthesized by dissolving polymer and salt in an appropriate solvent, say, acetonitrile, and the polymer electrolyte is recovered by evaporating the solvent. Thus, polymeric electrolyte is a solid solution of ions, either simple inorganic or more complex organic ions, in a polymeric matrix. The polymer chain must be able to solvate ions and simultaneously allow for ionic mobility in order to result in appreciable ionic conductivity. Polyethers, in particular, poly(ethylene oxide) $[PEO-(CH_2CH_2O)_n-]$ meet these two requirements, where the oxygen atoms coordinate to Li^+ cations. The PEO chain makes a first neighborhood shell around a given Li^+ cation, but it is locally flexible enough for cations to be able to detach and jump to different coordination sites.[1–5]

Our present microscopic understanding of the structure and dynamics of polymer electrolytes is the result of a combined use of many spectroscopic techniques and computer simulations. A plethora of spectroscopic measurements of polymer electrolytes can be found, for instance, neutron scattering,[6–14] x-ray,[15–18] NMR,[19–22] infrared, and Raman investigations.[23–28] Computer simulations of pure PEO (Refs. 29 and 30) and polymer electrolyte containing LiI,[29–31] NaI,[32–34] $LiPF_6$,[35,36] $LiBF_4$,[37] $LiClO_4$,[38,39] and [1-alkyl-3-methylimidazolium]PF_6 ionic liquids[40] have been reported. In a previous publication,[41] we provided a molecular dynamics (MD) investigation of salt concentration and temperature effects on the equilibrium structure of PEO/$LiClO_4$. The MD simulations were performed with a united atom model for the PEO chain, in which hydrogen atoms are not explicitly considered. The model was validated by the reasonable agreement between experimental and calculated static structure factor $S(k)$. An interesting finding of these MD investigations was the occurrence of a low-wave vector peak in $S(k)$ upon addition of $LiClO_4$ in PEO. This low-k feature in $S(k)$ has also been obtained by neutron scattering spectroscopy of PEO/$LiClO_4$,[8] although not as pronounced as in the MD calculated $S(k)$, and indicates that an extended-range order develops in the polymer electrolyte.

In this work, we investigate the dynamical properties of the simulated PEO/$LiClO_4$ polymer electrolyte. On a microscopic view, PEO/$LiClO_4$ dynamics has been revealed by NMR,[20] light scattering,[42] and quasielastic neutron scattering spectroscopy.[9] It will be shown that the united atom model for PEO is a reasonable one concerning dynamical properties with proper to good agreement between experimental and calculated intermediate scattering functions $F(\mathbf{k},t)$. By choosing an appropriate range of wave vector modulus k, $F(\mathbf{k},t)$ probes density fluctuations at different spatial ranges, allowing us to follow the time range of structural relaxation of the melt. In line with experimental findings on PEO/$LiClO_4$,[7,9] and also with previous MD simulations of PEO/LiI,[43] a remarkable slowing down of structural relaxation was observed upon addition of $LiClO_4$ in PEO. The fundamental transport coefficient of a polymer electrolyte, namely, ionic conductivity, has been calculated as a function of temperature and $LiClO_4$ concentration. The local environment in which Li^+ cations are immersed is made by the coordination of oxygen atoms from PEO chains and ClO_4^- anions. This implies anisotropy in cation motion, so that MD simulations reveal the interplay between structure and dynamics in PEO/$LiClO_4$.

II. COMPUTATIONAL DETAILS

The MD simulations were performed with a united atom model, in which hydrogen atoms of the PEO chain are not explicitly considered. All of the potential parameters can be

---

[a] Electronic mail: mccribei@ig.usp.br

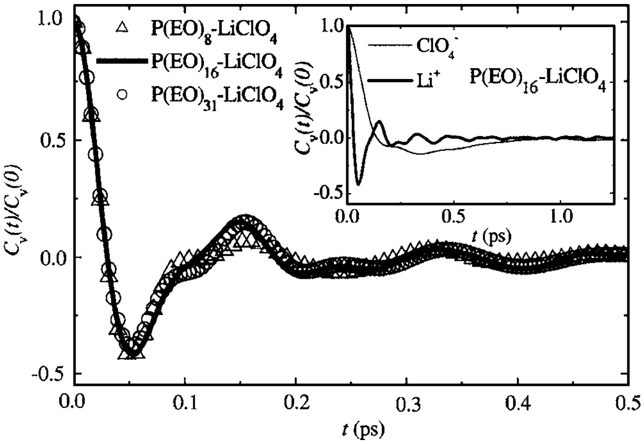

FIG. 1. Concentration dependence of the cation velocity time correlation function of PEO/$LiClO_4$ at 373 K. The inset shows Li^+ and ClO_4^- correlation function of $P(EO)_{16}-LiClO_4$ at 373 K.

found in the previous publication,[41] and they will not be repeated here. Briefly, the potential model for PEO includes inter- and intramolecular contributions. Intermolecular terms contain Lennard-Jones plus electrostatic interactions, with the latter being represented by partial charges assigned to the atomic sites of the PEO chain and the ClO_4^- anion. Li^+ cations carry their formal +1 charge. Intramolecular contributions in the PEO chain contain quadratic terms for bending plus dihedral angle terms. The C–C and C–O bond lengths, and the T_d symmetry of the ClO_4^- anion, were kept fixed by using the RATTLE algorithm.[44] No polarization effects were considered in the models.

The simulated systems contain 30 chains of $CH_3CH_2O(CH_2CH_2O)_{25}CH_2CH_3$, corresponding to a PEO model of molecular weight of 1174. Three different concentrations were simulated, where the $O_{polymer}:Li^+$ proportion were 7.8:1, 15.6:1, and 31.2:1. For brevity of notation, we will call these solutions of decreasing $LiClO_4$ concentration as $P(EO)_8-LiClO_4$, $P(EO)_{16}-LiClO_4$, and $P(EO)_{31}-LiClO_4$, respectively. The production of starting configurations was described in the previous publication.[41] Equilibration runs for pure PEO and PEO/$LiClO_4$ mixtures were, respectively, 1.0 and 2.0 ns long. Production runs not less than 2.0 ns long were performed in a cubic cell of fixed size at 363 K for pure PEO and 373 and 500 K for PEO/$LiClO_4$. This rather high temperature of 500 K was chosen in order to make the temperature effect on the simulated system clear. The Berendsen thermostat[45] was kept turned on during production runs with a small system-bath coupling parameter (1.0 ps). The Ewald sum method was used for handling long-range Coulomb interactions.[44] Further computational details can be found in the previous publication.[41]

III. RESULTS AND DISCUSSION

Figure 1 shows the dependence on salt concentration of the velocity time correlation functions of cations $C_v(t) = \langle \mathbf{v}_i(t) * \mathbf{v}_i(0) \rangle$ for PEO/$LiClO_4$ at 373 K. The inset compares the $C_v(t)$ of Li^+ and ClO_4^- at the intermediate concentration. It is clear that the pronounced oscillatory pattern in $C_v(t)$ is due to the short-time rattling dynamics of the ions in a temporary cage made by their first coordination shell, in particular, for Li^+ cations, because of the relatively low mass. The short-time dynamics is more easily appreciated in the corresponding vibrational density of states (DOS) obtained by Fourier transforming $C_v(t)$. Figure 2 shows the calculated DOS of anions and cations as a function of the $LiClO_4$ concentration at a fixed temperature. At low wave number, anion and cation DOSs overlap, the former being confined up to 200 cm^{-1}, whereas the latter extends to relatively high wave numbers. The overlapping dynamics of cations and anions at similar frequency ranges points to coupled (short-time) ionic motions. The salt concentration effect on calculated DOS is observed as a shift of anion DOS to higher frequency, and an overall broadening of the bands, with increasing $LiClO_4$ concentration. Broader bands suggest less homogeneous local environments around ionic species with increasing salt concentration. This finding is in line with Fig. 8 of Ref. 41, where we showed that the number of ionic pairs and aggregates in PEO/$LiClO_4$ at 373 K increases with salt concentration. In other words, sharper peaks in calculated DOS at a low concentration system reflect a more homogeneous environment experienced by the ions in a diluted solution of $LiClO_4$ in PEO.

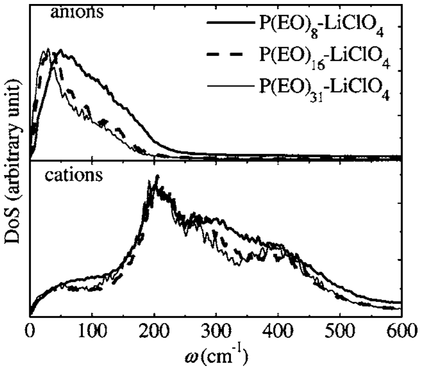

FIG. 2. Concentration dependence of the density of vibrational states of anions (top panel) and cations (bottom panel) of PEO/$LiClO_4$ at 373 K.

Interestingly, the broad high frequency band in cation DOS is clearly resolved into three peaks at 200, 300, and 400 cm^{-1} (Fig. 2). Thus, an obvious issue is to reveal the nature of distinct Li^+ short-time dynamics in PEO/$LiClO_4$. In order to assign the origin of the three high-ω peaks in cation DOS, we projected the vector $\mathbf{v}_i(t)$ of Li^+ cations onto distinct directions as depicted in Fig. 3. One direction is along the vector joining a given Li^+ and the nearest neighbor oxygen atom of a surrounding ClO_4^-. A given oxygen atom of ClO_4^- is considered first neighbor as long as the Li^+–O distance is smaller than 3.0 Å, according to the corresponding partial radial distribution function $g_{\alpha\beta}(r)$ (see Fig. 6 in Ref. 41). Similarly, the $\mathbf{v}_i(t)$ of Li^+ cations was projected along the direction joining a given Li^+ cation and neighboring oxygen atoms of the polymer chain. A subgroup of oxygen atoms of PEO whose distance to any Li^+ cation is smaller than 2.5 Å, which encompasses the first peak of the corresponding $g_{\alpha\beta}(r)$, and also another subgroup of oxygen atoms in a spherical shell around Li^+ cations with radius between

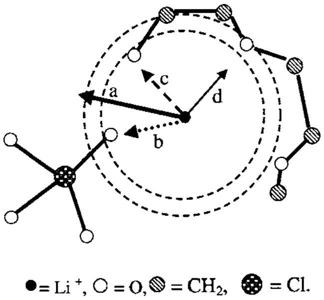

FIG. 3. Projections of the vector $\mathbf{v}_i(t)$ of a given Li$^+$ cation (the vector **a**) onto the direction of nearest neighbor oxygen atom of ClO$_4^-$ (the vector **b**) and the direction of PEO oxygen atoms within the first neighborhood shell (vectors **c** and **d**).

$2.5 < r_{\text{Li–O}} < 3.8$ Å were considered. These projected cation DOSs are shown in Fig. 4 for P(EO)$_{16}$–LiClO$_4$ at 373 K, where the original cation DOS of Fig. 2 is superimposed for comparison purpose. It is clear from Fig. 4 that relatively sharp bands with well-defined peaks are obtained with the projected velocities, with the higher frequency component of the original DOS being the result of short-time Li$^+$ dynamics along the anion direction. Absorption bands at ca. 400 cm^{-1} have been observed in far-infrared spectra of PEO/LiCF$_3$SO$_3$,[46] where they have also been assigned to Li–O cage modes. In line with the conclusions of Ref. 46, the projected motion of a *single* Li$^+$ in the simulated systems indicates that these bands do not arise from two populations of Li$^+$ belonging to different environments. The components at lower wave number in cation DOS are in the same frequency range encompassing the angle bending and dihedral torsion modes of the PEO chain as suggested by Raman investigations of polymer electrolytes.[2,28] Thus, cation short-time dynamics is strongly coupled with local motions of the polymeric chain as has been revealed by NMR investigations on PEO/LiBF$_4$.[20]

Figure 5 shows ionic mean square displacement (MSD) $\langle|\mathbf{r}_i(t)-r_i(0)|^2\rangle$ for P(EO)$_{16}$–LiClO$_4$ at 373 K. From the linear diffusive regime of MSD at long time, corresponding diffusion coefficients D were obtained, which are given in Table I. The calculated Li$^+$ cation D agrees with the experimental value reported for P(EO)$_8$–LiClO$_4$ at 373 K as obtained by NMR spectroscopy.[47] Overall, the magnitude of calculated D for PEO/LiClO$_4$ is consistent with MD results of PEO/LiI (Ref. 43) and NMR data for PEO/LiCF$_3$SO$_3$.[48]

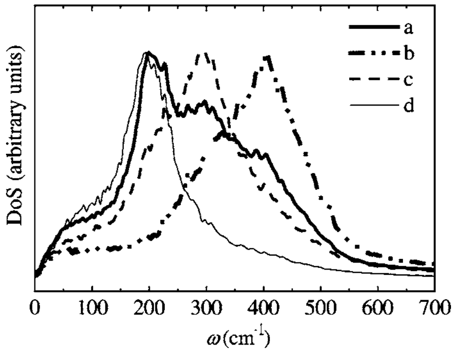

FIG. 4. Cation vibrational density of states: total (a) and projected onto the direction of vectors **b**, **c**, and **d** as defined in Fig. 3.

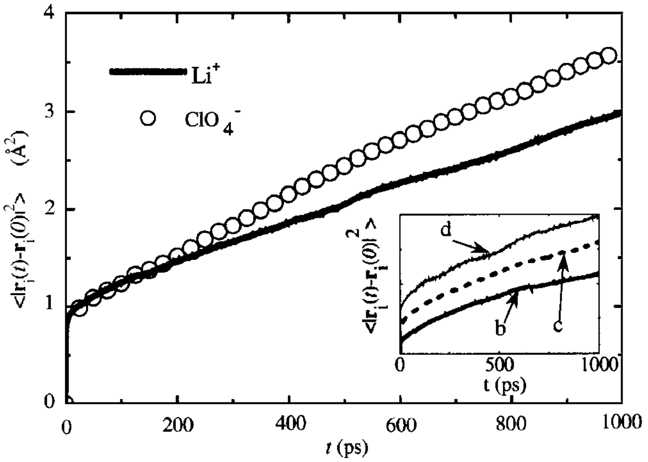

FIG. 5. Mean square displacement of Li$^+$ and ClO$_4^-$ of P(EO)$_{16}$–LiClO$_4$ at 373 K. The inset shows Li$^+$ mean square displacement projected onto directions **b**, **c**, and **d** as defined in Fig. 3.

Inspection of Table I indicates similar D values for anions and cations in a given temperature, suggesting coupled motion of both the species. Evidently, D increases with temperature, but it is worth noting that the relative increase of D with temperature is less pronounced in the case of the concentrated system P(EO)$_8$–LiClO$_4$. Furthermore, in the case of P(EO)$_8$–LiClO$_4$, the calculated D of oxygen atoms of PEO chain is similar to ionic D. Thus, the concentration and temperature dependences of calculated D strongly suggest increased coupling between ionic and polymer mobility with salt concentration. The inset in Fig. 5 shows the calculated MSD of Li$^+$ cations in P(EO)$_{16}$–LiClO$_4$ at 373 K, where the ionic displacement was projected either on the direction of neighboring oxygen atoms of PEO chains or ClO$_4^-$ anions (see Fig. 3). It is clear from the inset of Fig. 5 that Li$^+$ displacement towards O$_{\text{polymer}}$ atoms is enhanced in comparison to the O$_{\text{anion}}$ atoms. This finding is fully consistent with the distinct peak position observed in the DOS when cation $C_v(t)$ was projected along the PEO or the ClO$_4^-$ direction (see Fig. 4). The very distinct time ranges of Figs. 4 and 5 are worth mentioning, since $C_v(t)$ decays in a subpicosecond scale, whereas MSD is a long-time result of hundreds of picoseconds. Of course, D is related to the integral of $C_v(t)$ by a Green-Kubo equation,[49,50] so that Figs. 4 and 5 together show how a more defined rattling (higher frequency) motion of Li$^+$ cation along a given direction implies a relative hindrance on its displacement, which decreases long-time ionic diffusion along this direction.

Upon inspection of individual ionic trajectories, one identifies some Li$^+$ cations performing hopping between distinct sites in a relatively short-time event and some Li$^+$ cations following successive diffusive steps. Recently, the contribution of different mechanisms acting on cation mobility in PEO/LiTFSI has been quantified by MD simulations.[51] Cations in subdiffusive regime moving along PEO chains, cations moving together with PEO segments, and cations displaying hopping from a–(CH$_2$CH$_2$O)–segment to another have been identified. In the previous work,[41] we showed that

TABLE I. Diffusion coefficients D in 10^{-7} cm^2 s^{-1} of PEO/LiClO$_4$ at 373 and 500 K.

	Li^+		ClO_4^-		$O_{polimer}$	
	373 K	500 K	373 K	500 K	373 K	500 K
$P(EO)_8-LiClO_4$	0.16[a]	0.26	0.11	0.24	0.17	0.57
$P(EO)_{16}-LiClO_4$	0.32	4.31	0.44	3.45	1.12	10.41
$P(EO)_{31}-LiClO_4$	2.02	7.49	2.38	7.32	5.83	19.17

[a]The experimental value is 0.19×10^{-7} cm^2 s^{-1} (Ref. 47).

Li^+ cations are typically surrounded by five oxygen atoms, where three of them come from the PEO chain and two come from anions (see Fig. 7 in Ref. 41). Here, we stress the interplay between structure and dynamics in PEO/LiClO$_4$ by following the changing environment as a given Li^+ cation diffuses. The top panel in Fig. 6 shows the displacement of an arbitrary Li^+ cation whose diffusion mechanism is characterized by small diffusive steps. The bottom panel in Fig. 6 shows that the local environment around this cation is first rich in oxygen atoms from anions and poor in oxygen atoms from the PEO chain. When Li^+ diffusion starts at ca. 1.0 ns, the environment changes since the coordination of anions decreases and the coordination of the PEO chain increases. The case of a Li^+ cation in a polymer-rich, anion-poor environment, is shown in Figure 7, in which one sees hopping events between different sites. It is seen in Fig. 7 how the coordination changes when the Li^+ cation performs a jump. Fig. 7 also shows that the dihedral OCCO angle in the immediate neighborhood around the Li^+ cation is allowed to reach large values when the cation looses the polymer coordination. For comparison purposes, Fig. 8 shows a typical OCCO dihedral angle evolution in the case of pure PEO and $P(EO)_{16}-LiClO_4$. It is clear that the polymer chains are much more flexible in pure PEO, so that dihedral angles acquire large values in pure PEO more often. We already showed that the population of dihedral angles in *gauche* conformation increases, and the radius of gyration decreases, upon addition of LiClO$_4$ in PEO.[41] Thus, results shown in Figs. 7 and 8 are the dynamical counterpart of the changing conformation of PEO chains in the polymer electrolyte.

The time evolution of structures is probed by space and time correlation functions, such as the van Hove correlation function $G(r,t)$,[49,50]

$$G(r,t)=\left\langle \sum_i \sum_j \delta[\mathbf{r}+\mathbf{r}_i(t)-\mathbf{r}_j(0)]\right\rangle, \tag{1}$$

where $\mathbf{r}_i(t)$ is the position of particle i at time t. The self term $G_s(r,t)$ and the distinct term $G_d(r,t)$ are obtained from Eq. (1) provided that $i=j$ or $i\neq j$, respectively. The top panel of Fig. 9 shows the partial cation $G_s(r,t)$ of $P(EO)_{16}-LiClO_4$ at 373 K. The calculated $G_s(r,t)$ reveals the relatively slow ionic mobility. However, the 1.0 ns time range is long enough for the relaxation of cation $O_{polymer}$ structures, as revealed by the corresponding partial $G_d(r,t)$ (bottom panel in Fig. 9), whose main peak is almost completely washed out after 1.0 ns. The most important conclusion drawn from the comparison between the two panels of Fig. 9 is that the relaxation of $Li^+-O_{polymer}$ coordination takes place in half a nanosecond, but it does not necessarily imply that cations travel large distances in this time range.

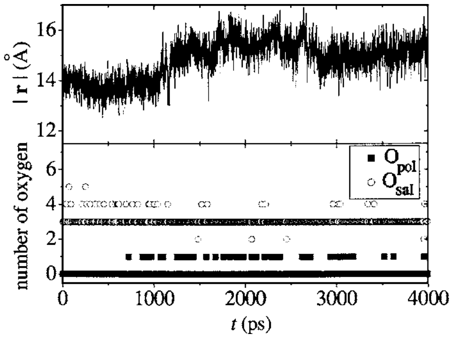

FIG. 6. Time evolution of the position of an arbitrary Li^+ cation (upper panel) and its local environment in $P(EO)_{16}-LiClO_4$ at 373 K (bottom panel): oxygen atoms from PEO and ClO_4^- within shells of radii of 3.8 and 3.0 Å, respectively.

The time scale of structural relaxation is more easily revealed by the intermediate scattering function $F(\mathbf{k},t)$, which probes density fluctuations at different spatial scales as selected by the wave vector modulus k. Instead of Fourier transforming $G(r,t)$, we calculate $F(\mathbf{k},t)$ directly from its definition,[49,50]

$$F(\mathbf{k},t)=\left\langle \sum_i \sum_j e^{i\mathbf{k}\cdot\mathbf{r}_i(t)-\mathbf{r}_j(0)]}\right\rangle. \tag{2}$$

The self term $F_s(\mathbf{k},t)$ calculated for pure PEO at 363 K is

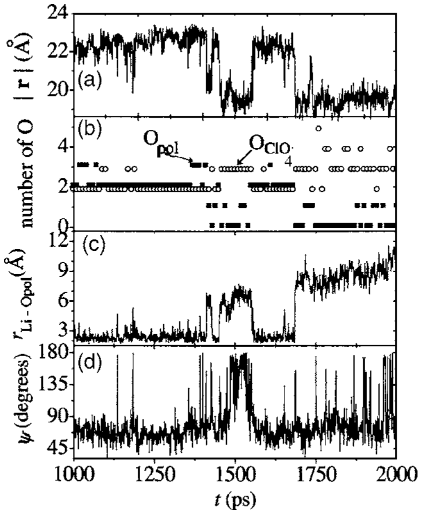

FIG. 7. Time evolution of a Li^+ cation position (panel a) and its local environment in $P(EO)_{16}-LiClO_4$ at 373 K: oxygen atoms from PEO and ClO_4^- within shells of radii of 3.8 and 3.0 Å, respectively (panel b), the $Li^+-O_{polymer}$ distance (panel c), and the OCCO dihedral angle of a segment of PEO chain coordinate to the cation (panel d).

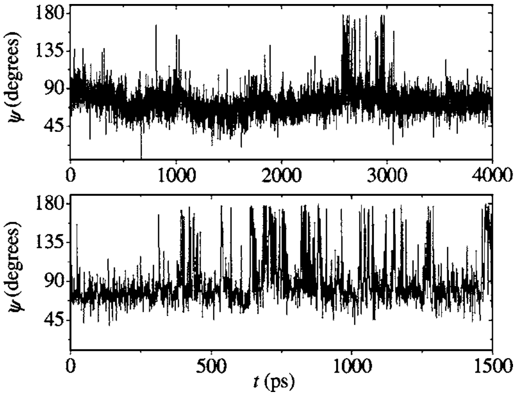

FIG. 8. Time evolution of arbitrary OCCO dihedral angles in P(EO)$_{16}$–LiClO$_4$ at 373 K (top panel) and pure PEO at 363 K (bottom panel).

shown in Fig. 10, where one sees the good agreement with experimental data obtained by the neutron scattering spectroscopy of a PEO sample with 23 EO repeat units, i.e., $(–CH_2CH_2O–)_n$ where $n=23$.[52] Confident that the united atom model used in the MD simulations is a reasonable one concerning the structural relaxation of PEO, Fig. 11 compares structural relaxation in pure PEO and PEO/LiClO$_4$. The self term and the distinct term $F_d(\mathbf{k},t)$ for carbon and oxygen atoms of the polymer chains are shown in the top and bottom panels of Fig. 11, respectively. In line with other dynamical consequences of structural modifications as discussed above, there is a significant slowing down of the structural relaxation of PEO upon addition of LiClO$_4$. In fact, quasielastic neutron scattering investigations of PEO/LiClO$_4$ assigned the slow relaxation in the polymer electrolyte as the consequence of coordination to Li$^+$ cations.[9,12] In comparison with PEO/NaI,[34,52] the $F_s(\mathbf{k},t)$ of PEO/LiClO$_4$ decays slower due to the fact that Li$^+$–PEO coordination is tighter than Na$^+$–PEO coordination. Figure 11 shows that a stretched exponential function $\exp[-(t/\tau)^\beta]$ gives a satisfactory fit to calculated $F_s(\mathbf{k},t)$. In the case of pure PEO, calculated best fit parameters ($\tau=12.60$ ps, $\beta=0.50$) agree with experimental parameters ($\tau=15.20$ ps, $\beta=0.582$).[52] However, in the case of PEO/LiClO$_4$, the simulated system seems more rigid than suggested by neutron scattering spectroscopy.[7,9]

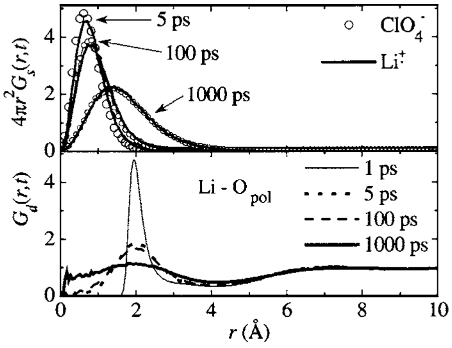

FIG. 9. Partial van Hove correlation functions of P(EO)$_{16}$–LiClO$_4$ at 373 K. Top panel: The self term; bottom panel: partial distinct term for Li$^+$–O$_{\text{polymer}}$ pairs.

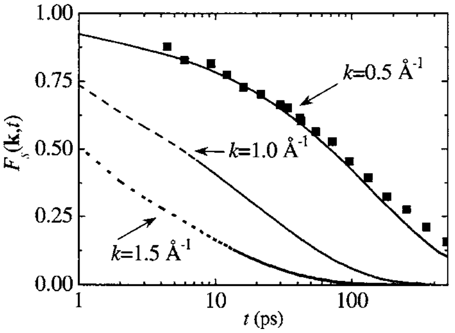

FIG. 10. Calculated (lines) and experimental (Ref. 34) (black squares) self term of the intermediate scattering function of pure PEO at 363 K.

Temperature and salt concentration effects on $F_s(\mathbf{k},t)$ are shown in Fig. 12. The more concentrated the PEO/LiClO$_4$ melt, the smaller the temperature effect on the decay of $F_s(\mathbf{k},t)$. Temperature and concentration effects on $F_s(\mathbf{k},t)$ follow diffusion coefficient data provided in Table I, since $F_s(\mathbf{k},t)$ decay is determined by D. Thus, in the limit of high LiClO$_4$ concentration, salt concentration effect seems to prevail over temperature effect in both structural and dynamical properties, since a relatively large increase in temperature does not break down the local order resulting from cation coordination[41] nor significantly fasten structural relaxation in PEO/LiClO$_4$.

Ionic conductivity κ, a collective dynamical property, was calculated by a collective version of the ionic MSD,[51]

$$\kappa = \lim_{t\to\infty} \frac{e^2}{6tVk_BT} \sum_{ij}^{N} z_i z_j \langle [\mathbf{r}_i(t) - \mathbf{r}_i(0)] \cdot [\mathbf{r}_j(t) - \mathbf{r}_j(0)] \rangle, \tag{3}$$

where e is the electron charge, V is the volume, T is the temperature, k_B is Boltzmann's constant, and z_i is the charge of ion i. Figure 13 illustrates collective MSD, i.e., the summation in Eq. (3), from which κ is obtained from the slope within the linear regime. The calculated κ are given in Table II, together with estimate from the Nernst-Einstein equation κ^{NE},[50]

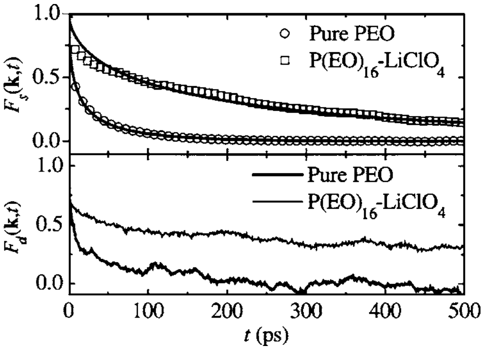

FIG. 11. Top panel: $F_s(\mathbf{k},t)$ at $k=1.0$ Å^{-1} of pure PEO at 363 K and P(EO)$_{16}$–LiClO$_4$ at 373 K: symbols are MD results and full lines are best fit with stretched exponential functions. Bottom panel: Corresponding $F_d(\mathbf{k},t)$ at $k=1.5$ Å^{-1}.

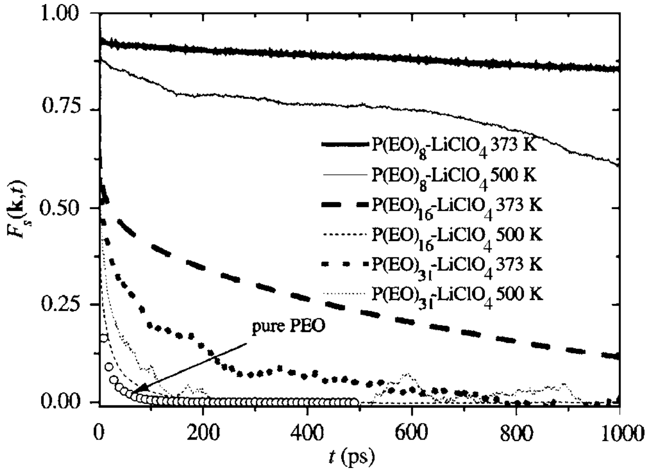

FIG. 12. Temperature and concentration effects on $F_s(\mathbf{k},t)$ of PEO/LiClO$_4$. For comparison purposes, the corresponding result in pure PEO at 373 K is shown by white circles.

$$\kappa^{\mathrm{NE}} = \frac{e^2}{kT}(\rho_- z_-^2 D_- + \rho_+ z_+^2 D_+), \tag{4}$$

where ρ_α is the number density of species α. The experimental κ goes through a maximum at intermediate concentrations,[54,55] a behavior that is clearly observed in simulated system only at 500 K. The simulated κ of PEO/LiI is about 10^{-4} S cm^{-1},[43] consistent with values obtained in this work. However, the simulated κ of P(EO)$_8$–LiClO$_4$ at 373 K is one order of magnitude lower than experimental κ,[47] as also observed in the MD simulation of PEO/LiI.[43] We calculated collective MSD up to 1.0 ns; unfortunately collective MSD curves were not shown in previous MD investigations[51] which could indicate that a change of slope in MSD might occur beyond this time range. However, this should not be the reason for the low κ in the simulated system, because we found κ lower than κ^{NE}, as one expects since κ^{NE} is an upper bound for the actual conductivity. Moreover, equilibration periods of 2.0 ns are typically used in MD simulations of polymer electrolytes. It could be instead that the low calculated value of κ is due to a too tight model for the polymer electrolyte, although the model properly reproduces the structural relaxation in pure PEO (see Fig. 10). A less rigid model might be achieved with the inclusion of polarization effects. Irrespective of concentration and temperature, κ^{NE} is approximately one order of magnitude higher than κ. Since the former is obtained from a single particle time correlation function, i.e., the single particle MSD, whereas the latter is a collective property, the ratio between κ^{NE} and κ indicates the relevance of cross correlation in ionic dynamics. Experimentally, similar differences between κ^{NE} and κ were also reported for PEO/LiPF$_6$.[53] It is worth mentioning that, for systems in which diffusion coefficients have been measured for both the cation and the anion species, for instance, PEO/LiPF$_6$,[53] it has been found that anion diffusion is greater than cation diffusion. In this work, however, similar Li$^+$ and ClO$_4^-$ diffusion coefficients have been obtained [see Table I and the $G_s(r,t)$ function in Fig. 9]. We have shown that a low-k peak, the so-called prepeak, develops in the calculated $S(k)$ upon addition of LiClO$_4$ in PEO.[41] This finding agrees with experimental data obtained by neutron scattering measurements,[8] although the calculated prepeak seems too intense in comparison with experiment. By calculating partial $S_{\alpha\beta}(k)$, we showed that the prepeak arises from spatial correlations between ionic species.[41] Even in diluted PEO/LiClO$_4$, the simulated systems present ionic pairs, which develop into ionic clusters at higher concentration. Since this structural feature seems enhanced in the simulations, in comparison with the real system, we interpret the calculated low values of κ, and the similar mobility for both ionic species, as a consequence of ionic pairing and clustering in the simulated PEO/LiClO$_4$ polymer electrolyte.

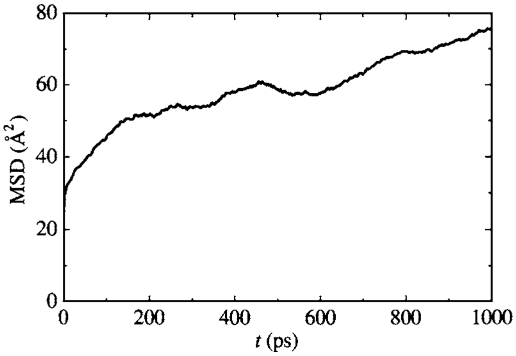

FIG. 13. Collective ionic MSD in P(EO)$_{16}$–LiClO$_4$ at 373 K.

IV. CONCLUSIONS

The present MD simulations have been performed with a model that provides a satisfactory account of both the equilibrium structure and dynamics of PEO as previously investigated by neutron scattering spectroscopy.[6,7,34] Concerning equilibrium structure of PEO, we showed in the previous work that the MD simulations reproduced experimental $S(k)$.[41] Concerning dynamical properties, it was shown in this work that calculated $F(\mathbf{k},t)$ agrees with experimental data for pure PEO. On formation of the polymer electrolyte, dynamical effects can be traced to the structural features revealed in the previous MD simulations,[41] either local changes, such as the increased population of dihedral angles in *gauche* conformation needed to embrace Li$^+$ cations, or the extended modification of the PEO chain as a whole, for instance, smaller radius of gyration. An interesting feature of PEO/LiClO$_4$ is that Li$^+$ cations are solvated by oxygen atoms from both the PEO chain and the ClO$_4^-$ anion. The non-

TABLE II. Calculated ionic conductivity κ in 10^{-4} S cm^{-1} of PEO/LiClO$_4$ at 373 and 500 K. κ^{NE} is the estimated conductivity according to the Nernst-Einstein equation, Eq. (4).

	κ		κ^{NE}	
	373 K	500 K	373 K	500 K
P(EO)$_8$–LiClO$_4$	0.21[a]	0.43	2.55	3.34
P(EO)$_{16}$–LiClO$_4$	0.43	2.70	3.40	25.88
P(EO)$_{31}$–LiClO$_4$	0.53	1.29	10.0	25.09

[a] The experimental value is 4.0×10^{-4} S cm^{-1} (Ref. 47).

equivalence of nearest neighboring oxygen atoms of PEO and ClO_4^-, as revealed by the corresponding radial distribution functions,[41] implies anisotropy in the Li^+ motions. The anisotropic short-time Li^+ dynamics is manifested as distinct peaks in the vibrational DOS. Consistent with the more intense first peak in the partial Li^+-O_{anion} than in the partial $Li^+-O_{polymer}$ $g(r)$ (see Fig. 6 in Ref. 41), the higher frequency band in the DOS was assigned to cation motion toward anions, whereas lower frequency bands were assigned to cation motion toward oxygen atoms of PEO chains. Interestingly, this anisotropy in short-time dynamics also manifests as a corresponding anisotropy in long-time diffusive dynamics. By following individual cations along their motion, it has been found that ionic mobility is strongly coupled with the time evolution of their local environment, as indicated by changing the coordination number of Li^+ by anions and polymer, and also the local conformation of PEO chains. In comparison with pure PEO, it has been found that the dihedral angles in PEO/$LiClO_4$ stay in *gauche* conformation for a longer period of time, i.e., PEO chains visit conformations with large dihedral angles more often in pure PEO than in the polymer electrolyte. Thus, PEO chains are more tight in the polymer electrolyte than in pure PEO, implying the slow down of structural relaxation in PEO/$LiClO_4$ as probed by $F(\mathbf{k},t)$. In the particular concentration and temperature in which experimental diffusion coefficient is available, calculated D_{Li+} agrees with the reported value.[47] In the simulated system, anion diffusion is comparable with cation diffusion, but corresponding experimental data for anions are not available. From diffusion coefficients, one predicts the Nernst-Einstein conductivity in PEO/$LiClO_4$ to be much higher than the actual conductivity calculated by the time correlation of charge current. However, the calculated conductivity is low in comparison with experimental data.[47] In the previous work,[41] we showed that an intermediate-range order develops in PEO/$LiClO_4$ as revealed by a low-k peak in the calculated $S(k)$. This finding is in line with neutron scattering measurements in PEO/$LiClO_4$,[8] but the intensity of such feature in calculated $S(k)$ seems too high in comparison with experimental $S(k)$. The calculated low conductivity, and similar diffusion coefficients for both the anions and the cations, should be also assigned to this structural feature since the low-k peak in $S(k)$ is due to ionic clustering in the bulk of the simulated system.[41] Thus, a remarkable interplay between structure and dynamics, both single-particle and collective dynamics, occurs in the polymer electrolyte PEO/$LiClO_4$.

ACKNOWLEDGMENTS

The authors acknowledge Dr. Sérgio M. Urahata and Dr. Oleg Borodin for helpful discussions. The computation facilities of LCCA at the Universidade de São Paulo are acknowledged. The authors are indebted to FAPESP and CNPq for financial support.

[1] F. M. Gray, *Polymer Electrolytes* (RSC Materials Monographs, Cambridge, 1997).

[2] J. R. MacCallum and C. A. Vincent, *Polymer Electrolyte Reviews-2* (Elsevier, London, 1989).

[3] J.-M. Tarascon, A. S. Gozdz, C. Schmutz, F. Shokoohi, and P. C. Warren, Solid State Ionics **86**, 49 (1996).

[4] K. Xu, Chem. Rev. (Washington, D.C.) **104**, 4303 (2004).

[5] J.-M. Tarascon and M. Armand, Nature (London) **414**, 359 (2001).

[6] B. K. Annis, O. Borodin, G. D. Smith, C. J. Benmore, A. K. Soper, and J. D. Londono, J. Chem. Phys. **115**, 10998 (2001).

[7] G. Mao, M.-L. Saboungi, D. L. Price, Y. S. Badyal, and H. E. Fischer, Europhys. Lett. **54**, 347 (2001).

[8] G. Mao, M.-L. Saboungi, D. L. Price, M. B. Armand, and W. S. Howells, Phys. Rev. Lett. **84**, 5536 (2000).

[9] G. Mao, R. F. Perea, W. S. Howells, D. L. Price, and M.-L. Saboungi, Nature (London) **405**, 163 (2000).

[10] P. Carlsson, J. Swenson, L. Borjesson, R. L. McGreevy, P. Jacobsson, L. M. Torell, and W. S. Howells, Electrochim. Acta **45**, 1449 (2000).

[11] A. Triolo, V. Arrighi, R. Triolo, S. Passerini, M. Mastragostino, R. E. Lechner, R. Ferguson, O. Borodin, and G. D. Smith, Physica B **301**, 163 (2001).

[12] M. L. Saboungi, D. L. Price, G. M. Mao, R. Fernandez-Perea, O. Borodin, G. D. Smith, M. Armand, and W. S. Howells, Solid State Ionics **147**, 225 (2002).

[13] J. A. Johnson, M.-L. Saboungi, D. L. Price, S. Ansell, T. P. Russel, J. W. Halley, and B. Nielsen, J. Chem. Phys. **109**, 7005 (1998).

[14] O. Borodin, R. Douglas, G. D. Smith, F. Trouw, and S. Petrucci, J. Phys. Chem. B **107**, 6813 (2003).

[15] W. A. Henderson, N. R. Brooks, W. W. Brennessel, and V. G. Young, Jr., J. Phys. Chem. A **108**, 225 (2004).

[16] Z. Gadjourova, Y. G. Andreev, D. P. Tunstall, and P. Bruce, Nature (London) **412**, 520 (2001).

[17] C. P. Rhodes and R. Frech, Macromolecules **34**, 2660 (2001).

[18] I. M. Litas, Y. G. Andreev, and P. G. Bruce, Chem. Mater. **14**, 2166 (2002).

[19] A. Asano, K. Takegoshi, and K. Hikichi, Polym. J. (Tokyo, Jpn.) **31**, 602 (1999).

[20] J. P. Donoso, T. J. Bonagamba, H. C. Panepucci, L. N. Oliveira, W. Gorecki, C. Berthier, and M. Armand, J. Chem. Phys. **98**, 10026 (1993).

[21] A. C. Bloise, C. C. Tambelli, R. W. A. Franco, J. P. Donoso, C. J. Magon, M. F. Souza, A. V. Rosário, and E. C. Pereira, Electrochim. Acta **46**, 1571 (2001).

[22] P. Mustarelli, E. Quartarone, C. Capiglia, C. Tomasi, P. Ferloni, and A. Magistris, J. Chem. Phys. **111**, 3761 (1999).

[23] H. C. Zhang, X. P. Xuan, J. J. Wang, and H. Q. Wang, Solid State Ionics **164**, 73 (2003).

[24] R. A. Sanders, A. G. Snow, R. Frech, and D. T. Glatzhofer, Electrochim. Acta **48**, 2247 (2003).

[25] I. Rey, J. C. Lassègues, J. Grondin, and L. Servant, Electrochim. Acta **43**, 1505 (1998).

[26] L. Edman, J. Phys. Chem. B **104**, 7254 (2000).

[27] M. Salomon, M. Z. Xu, E. M. Eyring, and S. Petrucci, J. Phys. Chem. **98**, 8234 (1994).

[28] L. Ducasse, M. Dussauze, J. Grondin, J. C. Lassegues, C. Naudin, and L. Servant, Phys. Chem. Chem. Phys. **5**, 567 (2003).

[29] O. Borodin and G. D. Smith, Macromolecules **31**, 8396 (1998).

[30] B. K. Annis, M. H. Kim, G. D. Wignall, O. Borodin, and G. D. Smith, Macromolecules **33**, 7544 (2000).

[31] B. A. Ferreira, F. Müller-Plathe, A. T. Bernardes, and W. B. De Almeida, Solid State Ionics **147**, 361 (2002).

[32] S. Neyertz and D. Brown, J. Chem. Phys. **104**, 3797 (1996).

[33] A. van Zon, B. Mos, P. Verkerk, and S. W. de Leeuw, Electrochim. Acta **46**, 1717 (2001).

[34] J. J. de Jonge, A. van Zon, and S. W. de Leeuw, Solid State Ionics **147**, 349 (2002).

[35] O. Borodin, G. D. Smith, and R. L. Jaffe, J. Comput. Chem. **22**, 641 (2001).

[36] A. Hektor, M. K. Klintenberg, A. Aabloo, and J. O. Thomas, J. Mater. Chem. **13**, 214 (2003).

[37] O. Borodin, G. D. Smith, and R. Douglas, J. Phys. Chem. B **107**, 6824 (2003).

[38] J. W. Halley, Y. Duan, L. A. Curtiss, and A. G. Baboul, J. Chem. Phys. **111**, 3302 (1999).

[39] Y. Duan, J. W. Halley, L. Curtiss, and P. Redfern, J. Chem. Phys. **122**, 054702 (2005).

[40] L. T. Costa and M. C. C. Ribeiro, J. Chem. Phys. **124**, 184902 (2006).

[41] L. J. A. Siqueira and M. C. C. Ribeiro, J. Chem. Phys. **122**, 194911 (2005).

[42] R. Walter, J. C. Selser, M. Smith, R. Bogoslovov, and G. Piet, J. Chem. Phys. **117**, 427 (2002).
[43] O. Borodin and G. D. Smith, Macromolecules **33**, 2273 (2000).
[44] M. P. Allen and D. Tildesley, *Computer Simulation of Liquids* (Claredon, Oxford, 1987).
[45] H. J. C. Berendsen, J. P. M. Postma, W. F. Gunsteren, A. DiNola, and J. R. Haak, J. Chem. Phys. **81**, 3684 (1984).
[46] V. Seneviratne, J. E. Furneaux, and R. Frech, Macromolecules **35**, 6392 (2002).
[47] W. Gorecki, R. Andreani, C. Berthier, M. Armand, M. Mali, J. Ross, and D. Brinkmann, Solid State Ionics **18–19**, 295 (1986).
[48] J. Shi and C. A. Vincent, Solid State Ionics **60**, 11 (1993).
[49] D. A. McQuarrie, *Statistical Mechanics* (University Science Books, Sausalito, 2000).
[50] J. P. Hansen and I. R. McDonald, *Theory of Simple Liquids* (Academic, London, 1990).
[51] O. Borodin and G. D. Smith, Macromolecules **39**, 1620 (2006).
[52] B. Mos, P. Verkek, S. Pouget, A. van Zon, G.-J. Bel, S. W. de Leeuw, and C. D. Eisenbach, J. Chem. Phys. **113**, 4 (2000).
[53] S. Aruguman, J. Shi, D. P. Tunstall, and C. A. Vincent, J. Phys.: Condens. Matter **5**, 153 (1993).
[54] A. Vallée, S. Besner, and J. Prud'Homme, Electrochim. Acta **37**, 1579 (1992).
[55] P. Ferloni, G. Chiodelli, A. Magistris, and M. Sanesi, Solid State Ionics **18&19**, 265 (1986).